Journal of Cereal Science 78 (2017) 10–18

Contents lists available at ScienceDirect

Journal of Cereal Science

journal homepage: www.elsevier.com/locate/jcs

The use of synchrotron X-rays and ultrasonics for investigating the bubble size distribution and its evolution in bread dough

Filiz Koksel [a, *], Anatoliy Strybulevych [b], Serdar Aritan [c], John H. Page [b], Martin G. Scanlon [d]

[a] 205 Ellis Building, 13 Freedman Crescent, Department of Food and Human Nutritional Sciences, University of Manitoba, Winnipeg, MB, R3T 2N2, Canada
[b] Department of Physics and Astronomy, University of Manitoba, Winnipeg, MB, R3T 2N2, Canada
[c] Biomechanics Laboratory, Hacettepe University, Ankara, Turkey
[d] Department of Food and Human Nutritional Sciences, University of Manitoba, Winnipeg, MB, R3T 2N2, Canada

ARTICLE INFO

Article history:
Received 1 November 2016
Received in revised form
10 May 2017
Accepted 30 June 2017
Available online 9 July 2017

ABSTRACT

The feasibility of using ultrasound as a tool for quantitatively measuring dough's bubbly microstructure was explored. The bubble size distribution (BSD) and its evolution due to disproportionation in non-yeasted doughs were characterized at the micron scale using synchrotron X-rays. Concurrently, measurements of the phase velocity and attenuation coefficient were performed using an ultrasonic transmission technique. An ultrasonic model based on propagation of sound waves in media with polydisperse scatterers was used to predict the wave vector from bubble microstructure definitions obtained microtomographically and compare it with the wave vector from measurement of velocity and attenuation. Correspondence was good across most of the frequency range, but a discrepancy between measured ultrasonic parameters and predictions from the model was observed in the low frequency region. A consideration of how resonating bubbles are sensitive to local rheological properties of the dough matrix was proposed as an important constituent for the ultrasonic model. Excellent predictions of the measured ultrasonic parameters were then attained across all frequencies. These results therefore show the potential of ultrasonic techniques for determination of BSDs in dough and their evolution, opening up the possibility of comprehensive in situ investigations of the mechanisms governing changes in dough's aerated structure during breadmaking.

1. Introduction

Dough aeration during mixing is crucially important, especially for mechanically developed doughs (Campbell et al., 1991), because the bubbles entrained during mixing are the only pooling points available for carbon dioxide to diffuse into during subsequent stages of the breadmaking process (Baker and Mize, 1941). Accordingly, aeration during mixing, and thus dough's bubbly structure, critically affects the cellular structure of the resulting loaf (Campbell et al., 2001, 1998, 1991). This relationship not only asserts the importance of knowledge of the size distribution of bubbles and their evolution in dough if high quality and consistent bread is to be produced, but also warrants investigation of the mechanisms governing changes in dough's aerated structure.

Deciphering how ingredients interact with mixing process parameters and understanding how these interactions affect the aerated structure of dough and bread are continuing challenges for food and cereal scientists (Koksel and Scanlon, 2012). One way to mitigate these challenges is to work with lean formula non-yeasted doughs (wheat flour, water, salt) (Létang et al., 2001). Furthermore, from a materials science perspective, these types of dough can be described as aerated soft solid systems where gravity-driven creaming of bubbles is absent (Mills et al., 2003), and thus understanding their bubble dynamics offers insights on gas exchange mechanisms that are relevant for a variety of bubbly materials.

Several techniques have been used for investigation of dough's microstructure and quantification of the bubble size distribution (BSD) in dough, including light microscopy (Carlson and Bohlin, 1978), magnetic resonance imaging (De Guio et al., 2009), confocal laser scanning microscopy (Upadhyay et al., 2012), and

* Corresponding author. 205 Ellis Building, 13 Freedman Crescent, Department of Food and Human Nutritional Sciences, University of Manitoba, Winnipeg, MB, R3T 2N2, Canada.
E-mail address: Filiz.Koksel@umanitoba.ca (F. Koksel).

http://dx.doi.org/10.1016/j.jcs.2017.06.022
0733-5210/

conventional bench-top X-ray microtomography (Bellido et al., 2006). However, the opacity of dough, as well as the fragility and the fast dynamics of bubbles [*e.g.*, doubling of median bubble size in less than an hour in the thin non-yeasted dough slices of Shimiya and Nakamura (1997)] have thwarted a characterization of the BSD in dough at the end of mixing by the aforementioned techniques. These techniques are also challenged to effectively monitor the changes in the microstructure of dough non-destructively and rapidly under bulk conditions. For example, using bench top X-ray microtomography, Bellido et al. (2006) reported that a 90 min long resting time after mixing was required to allow bubble dynamics to slow down. Only after this significant resting time, could images that were not blurred by the changes in bubbles be obtained (within a complete scan time of ~7 min). Because of its beam quality and brightness, X-ray radiation from a synchrotron source addresses these challenges, and so is very well-suited for scrutinizing the microstructure of optically opaque soft solids (Babin et al., 2008; Koksel et al., 2016a).

Another powerful technique for characterizing aerated soft solids is low intensity ultrasound (Leroy et al., 2008b), as a result of dramatic modification of wave propagation due to the presence of bubbles (Strybulevych et al., 2007). The effect of bubbles on acoustic propagation has been well documented for a long time in liquids (Carstensen and Foldy, 1947) and more recently in gels and viscoelastic media (Leroy et al., 2008a, 2008b; Strybulevych et al., 2007). Resonance of bubbles in dough is possible because both the density and compressibility of the dough matrix differ significantly from those of the gas in the bubbles (Koksel et al., 2014; Leroy et al., 2008a). The resonances of the polydisperse collection of bubbles present in dough lead to peaks in the frequency dependence of the ultrasonic phase velocity and attenuation coefficient. This frequency dependence can provide information on the distribution of bubble radii provided that a suitable model describing how ultrasonic phase velocity and attenuation coefficient are influenced by bubble resonance (Leroy et al., 2008a) is available, and the mechanical properties of the dough matrix are known (Leroy et al., 2011, 2008a).

Despite the sensitivity of acoustic parameters to the presence of bubbles in dough (Koksel et al., 2014; Strybulevych et al., 2012), the BSD in dough inferred from ultrasonic measurements (Leroy et al., 2008a) underestimated the median size of the BSD when it was compared with a BSD obtained microtomographically (Bellido et al., 2006) from a dough that had been sufficiently aged that the bubble disproportionation rate was slow. However, a direct comparison of the BSDs from the ultrasonic tests of Leroy et al. (2008a) and the tomographic tests of Bellido et al. (2006) is not entirely valid since dough samples had somewhat different dough formulations in the two studies. Accordingly, with the intention of exploring the capability of ultrasound as a tool for interrogating dough's bubbly structure, the objective of this study was to characterize the BSD (and its evolution due to disproportionation) in lean formula non-yeasted doughs as a function of time after mixing using X-rays from a synchrotron source, use it in an ultrasonic model to predict the wave vector, and compare it with the wave vector determined independently but simultaneously from measurements of phase velocity and attenuation coefficient obtained from an ultrasonic transmission technique.

2. Experimental

2.1. Sample preparation

The preparation of non-yeasted dough samples (200 g wheat flour, 136 g water and 4.8 g sodium chloride) by mixing at ambient pressure is described in Koksel et al. (2016a). In order to produce doughs with a lower bubble number density, dough samples were prepared at reduced pressure (Campbell et al., 1998), using the same formulation as the doughs prepared at ambient pressure. At reduced pressure, doughs were prepared using a GRL-200 pin mixer which was attached to a vacuum pump so that the headspace pressure during mixing was controlled (Elmehdi et al., 2004; Fan et al., 2013), allowing 2 min mixing at ambient pressure followed by 2 min mixing at reduced pressure. Three replicate doughs at ambient pressure and three replicate doughs at reduced pressure were prepared.

For doughs mixed at reduced pressure, from each of these three dough replicates, one subsample was tested ultrasonically while five subsamples were tested gravimetrically to determine dough density. For doughs mixed at ambient pressure, one subsample from each dough replicate was tested tomographically, another subsample was tested ultrasonically, and five subsamples were tested gravimetrically.

Dough subsamples were prepared for X-ray microtomography tests according to Koksel et al. (2016a). Only doughs mixed at ambient pressure were monitored tomographically. Dough subsamples were prepared for the ultrasonic tests (for doughs both mixed at ambient pressure and reduced pressure) according to Koksel et al. (2014).

2.2. Experimental methods

X-ray microtomography experiments were performed at the Canadian Light Source (Saskatoon, SK), at the Biomedical Imaging and Therapy beamline (BMIT-BM 05B1-1) which is suitable for the imaging of biological tissue. The sample scanning procedure and details of the image reconstruction were described by Koksel et al. (2016a). Image reconstruction and quantitative extraction of 3D features (explained with a flow chart in Fig. 1) start with acquiring projection images through 180°. A new image was acquired every 0.3° so that 600 projection images, each of which contains 3D spatial information built in 351 rows, were produced in each microtomography scan. Each microtomography scan (over 180°) took 2 min. The second step (Fig. 1) was acquisition of reference images to correct for nonuniformities in the X-ray beam. Two types of reference images were collected: flat and dark. Flat images were collected under the same condition as projection images but the sample was removed from the experimental hutch, while the dark images were collected under the same condition as projection images but both the sample and the X-rays were absent from the experimental hutch. The projection images were corrected using the flat and dark references. One row (out of 351) from each corrected projection image was rearranged to form one sinogram, so

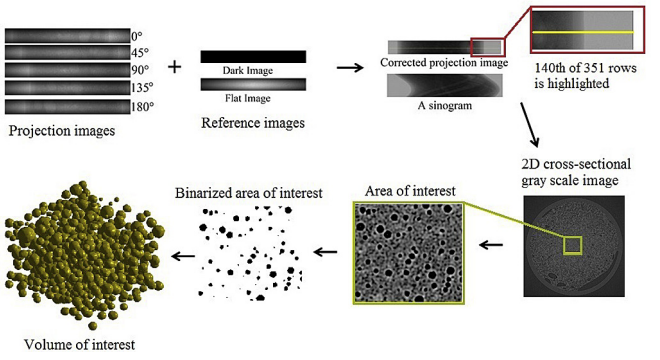

Fig. 1. Flow chart of image reconstruction and extraction of 3D features from X-ray microtomography experiments.

that a total of 351 sinograms were created. Each sinogram was backprojected to produce one 2D cross-sectional gray scale image of the dough sample with a resolution of 8.75 μm/pixel.

Out of the 351 2D cross-sectional grayscale images, two stacks – 100 slices each, one stack closer to the top and the other stack closer to the bottom section of the dough piece – were examined. An area of interest (at least 25,000 pixels) from the center of the 2D grayscale image was selected, and this area was binarized. Binarization of the tomography images involved selection of a threshold value so that the imaged void fraction of the dough sample matched the void fraction obtained from dough density measurements as described in Koksel et al. (2016a). Bubble cross sections (circles) were labelled based on their connectivity in consecutive slices (using a 6 point neighboring 3D connectivity criterion) and a 3D volume of interest was constructed (Koksel et al., 2016a).

Two ultrasonic pulse generator/receivers (Panametrics, Olympus NDT, Waltham, MA, USA), a pair of Panametrics transducers (Olympus NDT Waltham, MA, USA, central frequency: 2.25 MHz), and a digital oscilloscope (Tektronix Digital Phosphor Oscilloscope, model TDS5032B, Tektronix Inc., Beaverton, OR, USA) were used for ultrasonic measurements. The 2–3 mm thick dough subsample disc was placed between the two acrylic delay lines, one of which is in direct contact with the generating transducer and the other one with the receiving transducer. The subsample disk was squashed between the two delay lines to a thickness of 0.73 ± 0.01 mm in order to obtain good contact between the delay lines and the dough disc. This dough thickness was also small enough for the ultrasonic pulse at this central frequency to be measurable after travelling through the two acrylic delay lines and the dough subsample. The signal transmitted through the dough was averaged 500 times, recorded and analyzed to calculate the attenuation coefficient (α) and the phase velocity (v) as a function of frequency. In order to prevent moisture losses, and because of the temperature dependence of ultrasonic wave propagation, ultrasonic experiments were performed inside a cabinet (Caron Products and Services Inc., Model: Caron 6010, Marietta, OH, USA) at the beamline's workstation in which humidity (85 ± 1.0% relative humidity) and temperature (23 ± 0.1 °C) were kept constant.

The reference signal was created by placing the two acrylic delay lines in direct contact, with a small amount of industrial ultrasonic couplant (Sonotech Inc., WA, USA) between them, and the pulse transmitted through was recorded, averaged 500 times, and used as reference. The attenuation coefficient (α) and the phase velocity (v) were determined using Fourier analysis according to Koksel et al. (2014), and corrected for acoustic impedance differences at the dough-delay line interfaces (Leroy et al., 2011).

Bubble dynamics in the non-yeasted doughs were monitored both tomographically and ultrasonically (simultaneously) for 3 h following the end of mixing.

3. Results and discussion

3.1. Dough microstructure investigated by synchrotron radiation as a function of time after mixing

Structural properties of dough at micron resolution (8.75 μm/pixel) were obtained within a very short time (2 min/scan) owing to the high flux of X-rays from a synchrotron source (BMIT beamline of the Canadian Light Source). Dough samples were placed in the experimental hutch and scanned shortly after the end of mixing. Due to the rapid dynamics of bubbles right after mixing, the first clear 2D cross-sectional image was achieved at 36 min after mixing. Throughout the paper, this first scan at 36 min is referred to as the initial BSD. In Fig. 2, the initial BSD (36 min) in non-yeasted bread dough and its time evolution (76 min and 190 min) are presented. It is important to emphasize that the BSD in Fig. 2 is reported in bubble numbers following Shimiya and Nakamura (1997). Representing the size distribution of bubbles in terms of bubble volume fractions, instead of bubble numbers, is also a common practice in characterization of bubble sizes in bubbly foods [*e.g.*, see Babin et al. (2008), Campbell et al. (1991), Trinh et al. (2013)]. The widths of the bubble size ranges were chosen to allow sufficient numbers in a given range for statistical purposes, and only bubbles with radii greater than 16 μm were reported. In defining this lower bubble size limit, we have absolute certainty in the bubble sizes we report as a result of eliminating any bubble smaller than or equal to 25 connected voxels (conforming to the 6 point neighboring 3D connectivity criterion). Nevertheless, we acknowledge that relatively smaller bubbles ($R < 16$ μm) are likely to be present in the dough (Koksel et al., 2016a).

Due to the well focused X-ray radiation of the BMIT beamline, very large bubble number densities (number of bubbles/unit volume) were detected: of the order of approximately 50×10^{10} bubbles/m^3 at 36 min after completion of mixing. When the microstructure of non-yeasted doughs at the end of mixing is considered, the bubble number densities reported in this study are much higher compared to previous studies, *e.g.*, Campbell et al.'s (1991) number density of 33.1–78.5×10^9 bubbles/m^3 using microscopy and those of Bellido et al. (2006) – 30.4–56.5×10^9 bubbles/m^3 using bench-top X-ray microtomography.

Over the course of 3 h, the dough void fraction decreased; the decrease was slight and in a linear manner (from 11% ± 0.28 at 36 min to 9.2% ± 0.32 at 190 min). Concurrently, the bubble number density also decreased. This decrease in bubble number density with time accords with the findings of Leroy et al. (2008a) and Shimiya and Nakamura (1997). In our case, the decrease in the bubble number density was characterized by an exponential decay curve ($n = Ae^{-Bt}$, where n = number of bubbles per mm^3, $A = 645$ mm^{-3}, t = time after mixing (min) and $B = 0.00699$ min^{-1}, $R^2 = 0.994$).

The BSDs that were extracted from the 3D X-ray volumes were better characterized by lognormal distribution functions than by Gaussian ones. For example, at 190 min after the end of mixing, the goodness of fit for the lognormal characterization of the BSD was 0.99, while it was 0.92 for a Gaussian characterization. Accordingly, to characterize the initial BSD and its evolution with time, the lognormal probability density function, $N(R)$, was used:

$$N(R) = \frac{n}{\sqrt{2\pi}\varepsilon R}\exp\left[-\frac{(\ln R/R_0)^2}{2\varepsilon^2}\right] \quad (1)$$

where n, R, R_0 and ε are the bubble number density, bubble radius, median bubble radius and the width (polydispersity) of the lognormal BSD in the dough, respectively.

The median of the initial lognormal BSD was 22.1 ± 0.7 μm which increased to 24.0 ± 0.5 μm at 76 min and then to 29.2 ± 0.2 μm at 190 min. The increase in the median bubble size from 22.1 to 29.2 μm in approximately 2.5 h is an expected outcome of disproportionation, due to the diffusion of gas from relatively smaller to larger bubbles (Koksel et al., 2016a), an outcome also supported by the findings of Shimiya and Nakamura (1997) in their non-yeasted dough samples. The growth of median bubble radius with time is also consistent with the decrease in the bubble number density, since smaller bubbles shrink due to disproportionation and become smaller than our image resolution, shifting the median bubble size to larger values. We also draw attention to the high dispersity of the BSD. If the bubbles were monodisperse, a bubble number density of 50×10^{10} bubbles/m^3 and 11% gas volume fraction at 36 min after mixing would lead to a bubble size of

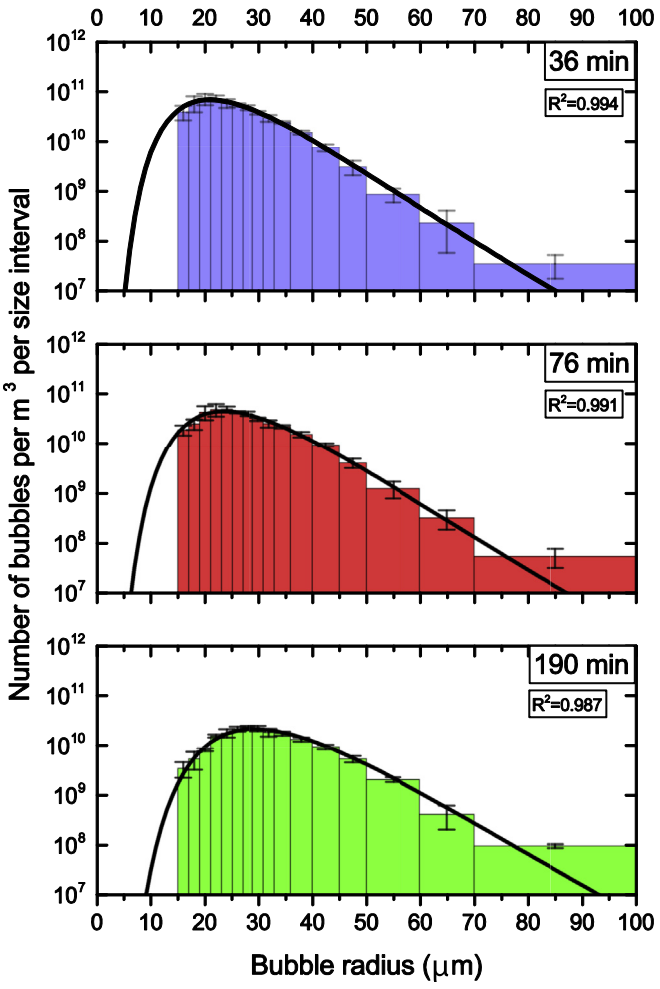

Fig. 2. The bubble size distribution (BSD) at 36 min (blue), 76 min (red), and 190 min (green) after the end of mixing. Solid black curves represent the lognormal fits to the BSDs. Lognormal distribution functions are fitted to the averages of 2 stacks (×3 replicates) for BSDs of 36 min, and 2 stacks (×2 replicates) for BSD of 76 and 190 min after the end of mixing. Error bars show ± SD of the 6 stacks for 36 min, and 4 stacks for 76 and 190 min.

~37 μm in comparison to the lognormal median bubble size of 22.1 μm. This wide range observed in bubble sizes can be captured by the use of synchrotron radiation since the high resolution images allow detection of small bubbles.

3.2. Dough microstructure investigated by the ultrasonic transmission technique

3.2.1. Ultrasonic parameters investigated by the transmission technique as a function of time after mixing

The phase velocity (v) and attenuation coefficient (α) are presented in Fig. 3a and b, respectively, for doughs mixed both at ambient and reduced pressure. Over the course of 3 h, at any given time after mixing, the doughs mixed at ambient pressure exhibited peaks spreading over the 500 kHz to 5 MHz region, whereas the ones mixed at reduced pressure lacked these peaks. From our dough density measurements, the ambient pressure dough subsamples contained approximately 11% volume fraction of bubbles, so the response of v and α as a function of frequency is typical of that of a bubbly medium (Leroy et al., 2008a). No peaks in v and α were observed for doughs mixed under reduced pressure, confirming that bubbles are a prerequisite for the characteristic signature of the frequency-dependent behavior of both v and α of wheat flour doughs (Fig. 3).

It is clear from Fig. 3a that the peak in v shifted to lower frequencies as time progressed. The relatively larger error bars, and thus the uncertainty at the resonance peak, are due to the difficulty in measuring very small phase shifts at large velocities. The changes in v with time were accompanied by a decrease in the peak magnitude in α and a shift in the peak to lower frequencies. These findings are characteristic of the time-dependent changes in non-yeasted doughs' bubbly structure due to disproportionation (Koksel et al., 2014; Leroy et al., 2008a; Strybulevych et al., 2012): mean bubble size increases as time progresses. Even though these findings are qualitative, they point to the sensitivity of ultrasonic measurements to the changes in the bubbly structure of dough observed from X-ray microtomography measurements where the median bubble size increased with time. As stated previously, for quantifying the changes in dough's bubbly structure, a suitable ultrasonic model describing how phase velocity and attenuation coefficient are influenced by bubble resonance (Leroy et al., 2008a) is needed (see the following section on the ultrasonic model).

For doughs mixed at ambient pressure, information at higher frequencies (>6 MHz) was obtained from the third harmonic of the central frequency of the ultrasonic transducers. At the high frequency end, v of the doughs mixed at ambient pressure leveled out so that a smaller value compared to the maximum velocity near resonances was attained that exhibited little dependence on post-mixing time (Fig. 3a). The time-invariant value of v at this high frequency is expected to correspond to the ultrasonic velocity in the dough matrix, v_0 (Leroy et al., 2011). This expectation is corroborated in light of results obtained from the doughs mixed at reduced pressure, where at 36 min after the end of mixing, the phase velocity was 1.91 ± 0.06 km/s (average v_0 ± standard deviation in the frequency range from 0.3 to 10 MHz). A slightly higher velocity (1.95 ± 0.06 km/s) was obtained at 180 min.

As expected, ultrasound propagation in the presence of bubbles is substantially affected due to resonant scattering. At lower frequencies (≪1 MHz well below the resonance frequency of bubbles), velocity of ultrasound in doughs mixed at ambient pressure was lower compared to that in doughs mixed at reduced pressure due to the large compressibility of bubbles (Koksel et al., 2016b; Strybulevych et al., 2007).

3.2.2. Ultrasonic model used to describe wave propagation in dough

Bread dough is a bubbly medium with complex mechanical properties. It is a viscoelastic soft solid with a dough matrix that possesses a frequency-dependent complex shear modulus in which is embedded a polydisperse distribution of bubble sizes. For a bubbly medium (where the sound scatterer is a bubble), the effective wave vector (k) that governs the propagation of longitudinally polarized ultrasonic wave is predicted by (Leroy et al., 2011):

$$k^2 = k_0^2 + \int [4\pi N(R) dR f_s(\omega, R)] \quad (2)$$

where k_0 is the wave vector of the dough matrix (*i.e.*, a bubble-free dough), $N(R)$ is the BSD, and $f_s(\omega, R)$ is the bubble's scattering function that is dependent on ω, the angular frequency. The parameters (their definition, symbol, unit and estimates) of the ultrasonic model are presented in Table 1.

The BSD, $N(R)$, can be extracted from ultrasonic measurements of k and k_0 via equation (2), provided that $f_s(\omega, R)$ can be determined as a function of frequency. Measurements of the ultrasonic velocity and attenuation coefficient of dough permit the effective wave vector (k) to be calculated:

$$k^* = \frac{\omega}{v} + i\frac{\alpha}{2} \tag{3}$$

where k is complex [it has both real (ω/v) and imaginary ($\alpha/2$) parts]. The ultrasonic velocity in dough mixed at reduced pressure (v_0) is sufficient for determination of k_0 ($= \omega/v_0$) since the contribution of α_0 to k_0 is negligible. For a bubble of radius R, the complex scattering function is given by:

$$f_s^*(\omega, R) = \frac{R}{(\omega_0/\omega)^2 - 1 + i\Gamma} \tag{4}$$

where ω_0 is the resonance angular frequency, and Γ is the damping constant. The resonance angular frequency of a bubble of radius R in a viscoelastic medium is inversely proportional to R and is also influenced by the real part of the complex shear modulus of the dough matrix, G', and the density of the dough matrix, ρ_0. In viscoelastic media, ω_0 can be approximated as:

$$\omega_0 \approx \frac{1}{R}\sqrt{\frac{3\kappa P_0 + 4G'}{\rho_0}} \tag{5}$$

where κ and P_0 are the complex polytropic index and the static pressure of the gas in the bubbles, respectively (Leroy et al., 2011). Thermal ($= 3\Im(\kappa)P_0/\rho_0 R^2\omega^2$), viscous ($= 4G''/\rho_0 R^2\omega^2$) and radiative ($= Rk_0$) energy losses contribute to the damping constant, Γ.

The shear modulus of the dough matrix strongly affects the complex scattering function and thus ultrasonic wave propagation (Leroy et al., 2011; Strybulevych et al., 2012). It is evident from equation (5) that an increase in G' shifts ω_0 to higher frequencies, while an increase in the imaginary part of the matrix shear modulus, G'', increases the magnitude of Γ. For more background information on how the shear modulus of dough matrix affects the ultrasonic phase velocity and attenuation coefficient of bubbly media such as dough, readers are referred to Leroy et al. (2011) and Koksel et al. (2016b).

3.3. Relationship between measured effective wave vector and the ultrasonic model parameters

The validity of the ultrasonic model presented in Section 3.2.2. has been experimentally confirmed for dilute (*i.e.*, void fraction < 1%) bubbly liquids (Commander and Prosperetti, 1989; Wilson, 2005) and gels (Leroy et al., 2008b). In order to explore the capability of this ultrasonic model for examining dough's bubbly structure and the BSD in dough, the degree of correspondence between the effective wave vector calculated using v and α from ultrasonic measurements (equation (3)) and the effective wave vector predicted from the ultrasonic model (equation (2)) needs to be explored.

For prediction of the effective wave vector from the ultrasonic model, equation (2) is used. According to the ultrasonic model, the effective wave vector, k, depends on (*i*) the wave vector of the dough matrix, k_0, (*ii*) the bubble size distribution, $N(R)$, and (*iii*) the bubble's scattering function, $f_s(\omega, R)$. In this section, we focus on the significance of these individual components in terms of their contribution to k, calculating predictions of the model using independently measured or estimated parameters (best estimates available in the literature).

In equation (2), experimental ultrasonic measurements on doughs mixed at reduced pressure permit determination of k_0 as a function of frequency. Doughs mixed at reduced pressure minimize bubble occlusion during mixing so that k_0 of the bubble-free dough (*i.e.*, the dough matrix) can be determined through v_0 (and α_0). From Fig. 3, it is apparent that both v_0 and α_0 are essentially time independent during the timescale of the ultrasonic experiments (3 h). Doughs mixed at reduced pressure had an ultrasonic velocity of $v_0 \approx 1.9$ km/s. This essentially constant ultrasonic velocity in the bubble-free dough is in agreement with high frequency extrapolations of Koksel et al. (2014) and Létang et al. (2001). The attenuation coefficient in the dough matrix (α_0) is small and has a negligible contribution to the effective wave vector. Similar small values of α_0 in this frequency range were also reported by Fan (2007).

The second parameter that is needed for prediction of k from the ultrasonic model [equation (2)] is the BSD [$N(R)$]. The changes in the BSD as a function of post-mixing time were obtained from the

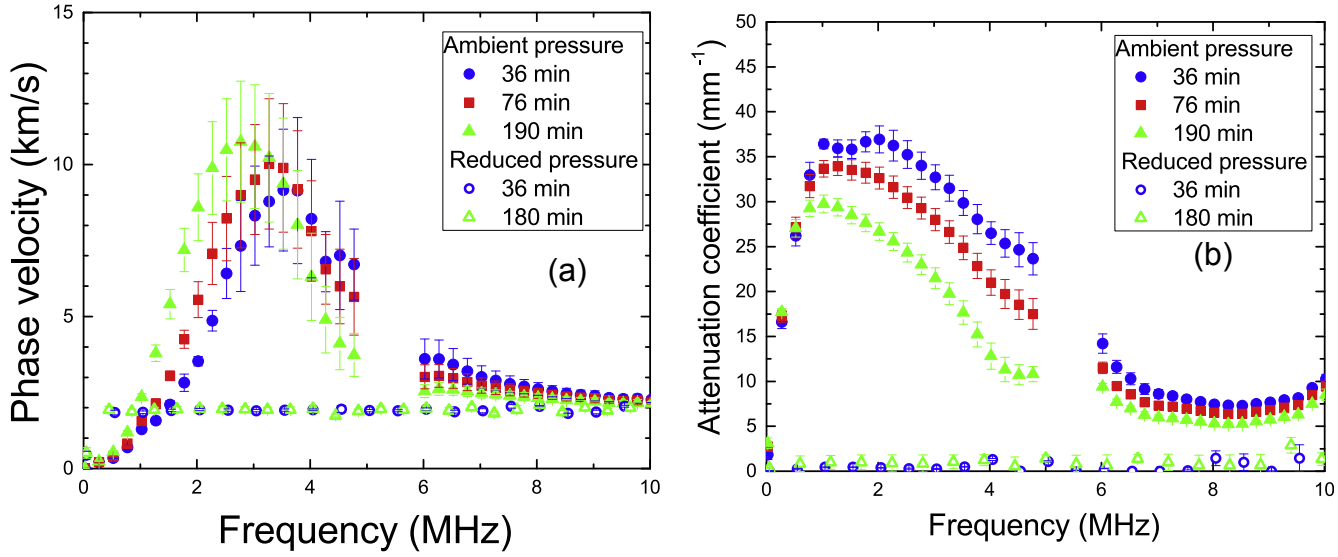

Fig. 3. Time dependence of (a) phase velocity, v, and (b) attenuation coefficient, α, for doughs mixed at ambient pressure (solid symbols, blue circles: 36 min, red squares: 76 min, green triangles: 190 min) and reduced pressure (open symbols, blue circles: 36 min, green triangles: 180 min) as measured by the ultrasonic transmission technique. Error bars (±1 SD) not seen if smaller than symbols.

Table 1
Parameters of the ultrasonic model.

Parameters	Symbols	Units (SI system)	Measurements/Estimates
Attenuation coefficient	α	m^{-1}	Up to 40 mm^{-1} (see Fig. 3b)
Phase velocity	v	ms^{-1}	Up to 13 km/s (see Fig. 3a)
Attenuation coefficient in dough matrix	α_0	m^{-1}	Below 5 mm^{-1} (see Fig. 3b)
Phase velocity in dough matrix	v_0	ms^{-1}	≈1.91 km/s (see Fig. 3a)
Bubble size distribution (BSD)	$N(R)$	m^{-4}	Lognormal (Koksel et al., 2016a)
Bubble number density	n	m^{-3}	At 36 min after mixing: 872 ± 134 bubbles/m^3 (Koksel et al., 2016a)
Bubble radius	R	m	At 90 min after mixing: 31–321 μm within 95.5% confidence interval (Bellido et al., 2006)
Median bubble radius of the BSD	R_0	m	In non-yeasted doughs: 7.5 μm at 3 min after mixing (Shimiya and Nakamura, 1997) 22.1 μm at 36 min after mixing (Koksel et al., 2016a) 50 μm at 90 min after mixing (Bellido et al., 2006)
Width (polydispersity) of the BSD	ε	dimensionless	In non-yeasted doughs: 0.18 at 3 min after mixing (Shimiya and Nakamura, 1997) 0.32 at 36 min after mixing (Koksel et al., 2016a) 0.63 at 90 min after mixing (Bellido et al., 2006)
Density	ρ	kgm^{-3}	≈1150 kgm^{-3} (Koksel et al., 2014) ≈1120 kgm^{-3} (current study)
Density of dough matrix	ρ_0	kgm^{-3}	≈1270 kgm^{-3} (Koksel et al., 2014) ≈1250 kgm^{-3} (current study)
Angular frequency	ω	rad/s	up to $\omega/2\pi = 10$ MHz in the current study
Resonance angular frequency	ω_0	rad/s	2.2 Mrad/s for a bubble with a radius of $R = 20$ μm in a matrix with a shear modulus of $G' = 0.49$ MPa (see below)
Effective wave vector	k	m^{-1}	Frequency dependent (see equation (3))
Effective wave vector of dough matrix	k_0	m^{-1}	Frequency dependent (see equation (3))
Bubble's scattering function	f_s	m	Frequency dependent (see equation (4))
Damping constant	Γ	dimensionless	$\Gamma = \Gamma_{thermal} + \Gamma_{viscous} + \Gamma_{radiative}$
Thermal losses	$\Gamma_{thermal}$	dimensionless	$\Gamma_{thermal} = 3\Im(\kappa)P_0/\rho_0 R^2\omega^2$
Viscous losses	$\Gamma_{viscous}$	dimensionless	$\Gamma_{viscous} = 4G''/\rho_0 R^2\omega^2$
Radiative losses	$\Gamma_{radiative}$	dimensionless	$\Gamma_{radiative} = Rk_0$
Complex shear modulus of dough matrix	G^*	Pa	$G^* = G' + iG''$
Real	G'	Pa	1.71 MPa at 2 MHz (adjusted G' in the current study) 0.49 MPa at 2 MHz (Leroy et al., 2010) 0.15 MPa at ~3 MHz (Létang et al., 2001)
Imaginary	G''	Pa	3.83 MPa at 2 MHz (adjusted G'' in the current study) 0.36 MPa at 2 MHz (Leroy et al., 2010) 0.06 MPa at ~3 MHz (Létang et al., 2001)
Polytropic index	κ	dimensionless	1.4 for air (Leroy et al., 2011)
Static pressure of the gas in the bubbles	P_0	Pa	≈Atmospheric pressure

X-ray microtomography measurements (Fig. 2). The time-dependent lognormal BSD parameters (R_0 and ε) from X-ray microtomography experiments were inputted to the ultrasonic model [equation (2)] for prediction of k. For example, at 36 min after the end of mixing, R_0 of 22.1 ± 0.7 μm and ε of 0.31 ± 0.01 were used to predict k.

The final parameter that is needed for the prediction of k from equation (2) is the bubbles' scattering function, $f_s(\omega, R)$. The bubbles' scattering function [equation (4)] depends on the resonance angular frequency [ω_0, equation (5)] and the damping constant (Γ). As previously mentioned in Section 3.2.2, the dough matrix shear modulus, both its real (G') and imaginary (G'') parts, substantially affects $f_s(\omega, R)$. For initial model predictions of k, the high frequency extrapolations of shear moduli measured by Leroy et al. (2010) were used ($G' = 10900\omega^{0.234\pm0.004}$, $G'' = 4300\omega^{0.271\pm0.005}$).

From model predictions of k, v and α are calculated. This v and α pair [the predicted v and α (red dashed curves)] and the experimental measurements of v and α (black square symbols) at 36 min after the end of mixing are presented in Fig. 4a and b. It is important to point out that there are no additional fitting parameters and that Fig. 4 represents a direct comparison of equation (2) with the experimental ultrasonic results.

At 36 min after the end of mixing, the agreement between experimental phase velocity values and the predictions of the ultrasonic model were very good at high frequencies (Fig. 4a). Below ~5 MHz, deviations from the experimental data were larger, because at the high velocities around the resonance peak the phase shift is more difficult to measure (Strybulevych et al., 2007) – see the larger error bars at the resonance peak in Fig. 3a. Comparison of the experimental attenuation coefficient to its ultrasonic model prediction showed excellent overall correspondence at frequencies above 2 MHz (Fig. 4b). However, deviations from experimental values were evident at lower frequencies. For both v and α, the discrepancy observed at the lower frequency end of the resonance peak indicates that either deficiencies in the ultrasonic model exist or there are uncertainties in the parameters used to predict v and α.

3.4. Critical examination of parameters in the ultrasonic model

In this section, we examine possible causes for the poorer model fit at lower frequencies by treating each component of the ultrasonic model individually. Since model prediction of the wave vector (equation (2)), and thus model predictions of v and α, were derived using the effective matrix wave vector (k_0), the BSD (*i.e.*, R_0 and ε) and the scattering function of bubbles [$f_s(\omega, R)$], uncertainties associated with each these components will be examined.

The effective matrix wave vector ($k_0 = \omega/v_0$) is a function of the ultrasonic velocity (v_0) in the bubble-free dough (*i.e.*, the dough matrix). As can be seen from Fig. 3, for dough mixed at reduced pressure, error bars are smaller than symbol size at all frequencies and both times for v. Since the wave vector of the bubble-free dough was calculated from doughs mixed at reduced pressure, k_0 contributes little to the discrepancy between the measured and predicted values for v and α in Fig. 4.

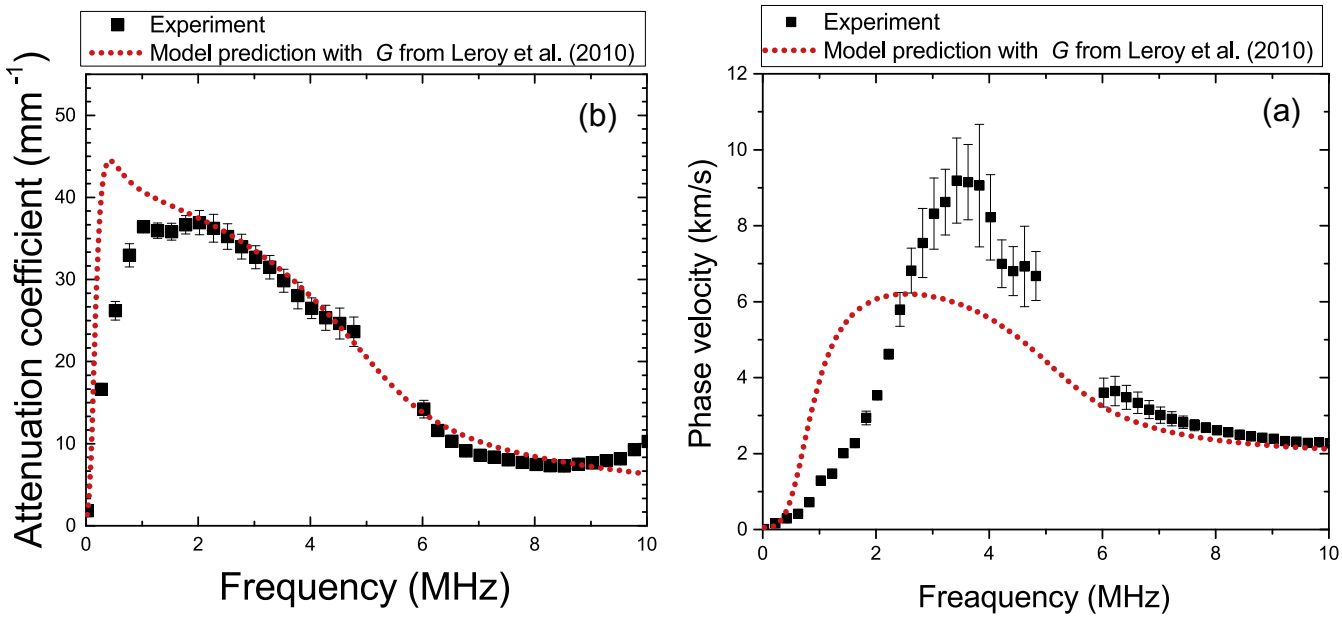

Fig. 4. Phase velocity (a) and attenuation coefficient (b) 36 min after the end of mixing. Black symbols: experimental values, red dashed curves: ultrasonic model predictions derived using R_0 and ε from X-ray microtomography images, dough matrix measurements from Fig. 3, and using high frequency extrapolations of shear moduli from Leroy et al. (2010).

The second plausible contributor to uncertainty in the ultrasonic model predictions is the BSD (R_0 and ε). In this study, ultrasonic and X-ray experiments were performed on subsamples from the same dough independently but simultaneously, permitting a direct comparison of ultrasonic and tomographic analyses. The goodness of fit values for the lognormal distribution to the bubble size distribution data (Fig. 2) are very close to 1, so R_0 and ε provide accurate representation of the BSD for equation (2) predictions of v and α.

On the other hand, we have previously reported that the lower confidence limit for bubble radius determination in our X-ray images was 16 μm [see section 3.1 and Koksel et al. (2016a)]. A bubble with a radius smaller than 16 μm represents a bubble that is formed by a contiguous clustering of a small number of voxels that is less than or equal to 25 [with a minimum 6 point neighboring 3D connectivity criterion (Koksel et al., 2016a)]. Therefore, do bubbles with radii <16 μm (that do not conform to the lognormal distribution) contribute to the mismatch of experimental and predicted k values? In order to test this hypothesis, the lower bubble radius limit of the BSD was assigned to 10 μm, and a different set of R_0 and ε values was derived to predict v and α from equation (2). The predicted v and α values were barely affected by the addition of bubbles that had radii between 10 and 16 μm (data not shown), and therefore these smaller bubbles are not responsible for the mismatch of measured and predicted v and α at the low frequency end of the resonance peak. This outcome was not a surprise given that the frequency at which a bubble resonates is inversely related to bubble radius (Strybulevych et al., 2007), and therefore adding smaller bubbles to the BSD will affect the higher frequency end of the resonance peak, not its lower frequency end.

Another uncertainty regarding R_0 and ε arises from how dough subsamples were handled for the X-ray tomography and ultrasonic experiments. While a dough subsample for an X-ray microtomography experiment was placed in a plastic container with minimal handling and deformation (Koksel et al., 2016a), a dough subsample for ultrasonic tests was squashed between the delay lines of the ultrasonic set-up. The high strains experienced by the dough during this squashing action (from 2 to 3 mm to <1 mm dough thickness) may very well affect the shapes and/or sizes of the bubbles. In future work, this uncertainty will be investigated through imaging dough samples that are compressed to various thicknesses and examining how bubble sizes, shapes, and their evolution are affected.

The third uncertainty is the bubble's scattering function, $f_s(\omega, R)$. The scattering function assumes that the response of bubbles in dough to the incoming ultrasound waves is not correlated to their positions. In addition, the void fraction in dough is ~10%, a value considerably higher than what has been experimentally validated for this model (Leroy et al., 2008b). An analysis of how resonance effects in one bubble affect resonance in a neighboring bubble has been given by Leroy et al. (2011) for a very simple aerated system. Given the complex nature of dough (where “hard” starch granules are embedded in a heterogeneous hydrated matrix) and the relatively high gas volume fraction in dough, more analysis is required to evaluate the effect of correlated bubble interactions on the effective wave vector, and hence the predicted v and α values.

The bubble's scattering function is also affected by dough matrix rheology. An increase in G' of the dough matrix affects $f_s(\omega, R)$ by shifting the resonance peak to higher frequencies (Leroy et al., 2008a) while an increase in G'' broadens the resonance peak (Leroy et al., 2011). In order to examine the contribution of G' and G'' to the frequency dependence of model predictions of $f_s(\omega, R)$, an iterative fitting procedure was performed. The fitting procedure was based on minimizing the deviation between measured and predicted k, by adjusting G' and G''. A least squares method was used to minimize the sum of squared difference between experimental values and ultrasonic model predictions, over the whole of the frequency range. Using the new values for G' and G'', the ultrasonic model predictions of v and α are presented in Fig. 5a and b, respectively. Very good correspondence was found between the measured and predicted velocity at 36 min after the end of mixing, except for the magnitude of the velocity peak in a limited frequency range around the resonance peak (red solid curve in Fig. 5a). For the attenuation coefficient, correspondence between the measured

values and model predictions was near-perfect at 36 min after the end of mixing (red solid curve in Fig. 5b).

The time dependence of the measured and predicted attenuation coefficient are presented in Fig. 5c and d for 76 min and 190 min after the end of mixing, respectively. The same outcome, as per 36 min, was observed for 76 min and 190 min: ultrasonic model predictions of α showed excellent overall correspondence, following the changes in the measured α that accompanied the evolution of the dough's bubbly structure, although with slight underestimation at the longest time (Fig. 5d).

The real and imaginary parts of the shear modulus that gave the closest predictions of the model to the measured data were higher than extrapolations of what has been reported in the literature to our frequency range (Table 1). A G' that is more than three times higher (1.71 MPa *vs.* 0.49 MPa at ~55 min after the end of mixing) and a G'' that is more than an order of magnitude higher (3.83 MPa vs. 0.36 MPa) than would be obtained based on an extrapolation of the results of Leroy et al. (2010) provided the best fit to our experimental data. While this difference in matrix rheological properties remains questionable, one plausible explanation is that the bulk rheological properties of bread dough (as measured by high frequency methods) differ from the local rheological properties in the vicinity of bubbles that are excited into resonance with incident ultrasound waves. In view of the structural complexity of the dough matrix that surrounds the bubbles in dough, the applicability of bulk rheological properties to describe local rheological properties in the region around an oscillating bubble should be carefully considered.

In a non-yeasted wheat flour dough system, while starch granules [mean granule size ~17 μm (Salerno et al., 2014)] and gas

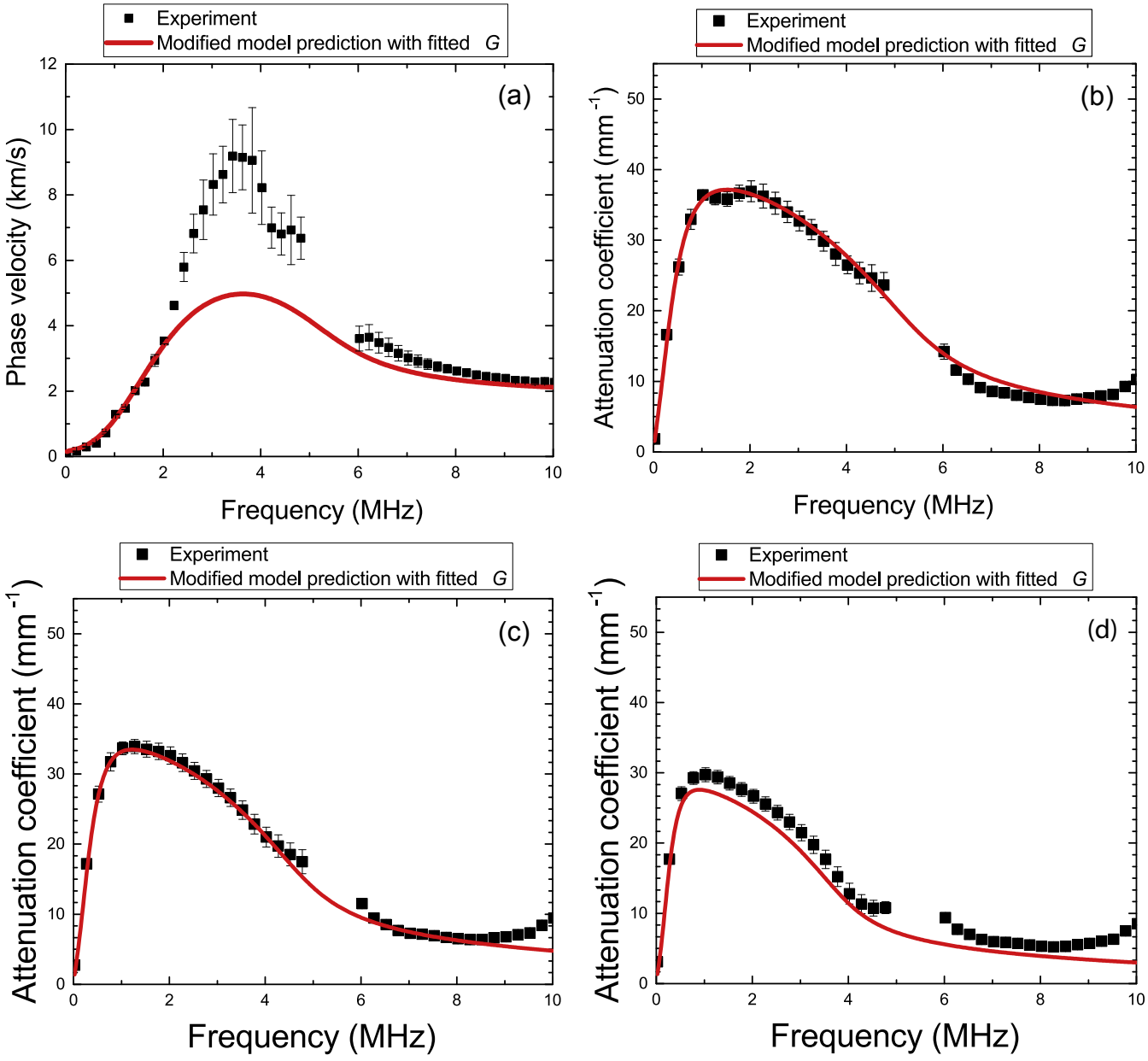

Fig. 5. Phase velocity (a), and attenuation coefficient (b) at 36 min after the end of mixing. Attenuation coefficient comparison at 76 min (c), and 190 min (d) after the end of mixing. Black symbols: experimental values, red solid curves: ultrasonic model predictions derived using R_0 and ε from X-ray microtomography images and using dough matrix shear moduli as adjustable fitting parameters.

bubbles are of comparable sizes, the volume fraction of starch granules [~60% of dough volume (Tanner et al., 2008)] is much greater than the volume fraction of gas bubbles (~11% in our case). This means that there will be more than one starch granule in the vicinity of an isolated bubble. Furthermore, rheological properties of the individual dough components differ, *e.g.*, stiff starch granules (Salerno et al., 2014) *vs.* the more compliant gluten matrix (Chichti et al., 2013). Accordingly, the movement of individual dough components under ultrasonic excitation at resonance is likely to differ. As bubbles resonate, the starch granules in the vicinity of bubbles will conceivably butt into each other as the dough is displaced at the surface of the resonating bubbles. As starch granules, which are much stiffer than the gluten matrix enveloping them, push into each other, they induce a stiffening of the local rheological properties. This local mechanism of granule-granule interaction, even though speculative, justifies the high values for the dough matrix shear moduli (Table 1) in the vicinity of bubbles during resonance compared to bulk rheology values.

Notwithstanding the limitations associated with a true definition of local rheological properties for the dough matrix, the ultrasonic model demonstrates notable agreement between the measured and predicted velocities and attenuation coefficients. Our results demonstrate the potential of the ultrasonic technique to noninvasively monitor the dynamics of changing bubble sizes in dough.

4. Conclusion

An ultrasonic transmission technique coupled with a model describing wave propagation in bubbly media has the potential to measure dough's microstructure in situ. The shear modulus of the dough matrix - both its real and imaginary parts contributing to how bubbles scatter sound in dough - had a substantial effect on model predictions. Based on considerations of local rheology in the vicinity of resonating bubbles, a near-perfect agreement between experimental data and model predictions was achieved using “large” values for the dough matrix shear modulus. Ultrasonic measurements therefore have the potential to determine bubble size distributions and their evolution in dough during breadmaking, notwithstanding the need to better define some of the parameters entering the model used to interpret the experimental data. Future work will focus on understanding the nature of microrheological changes in dough matrix at the bubble-dough matrix interface and its response to incident ultrasonic waves.

Acknowledgements

The authors would like to acknowledge University of Manitoba Graduate Fellowship (Canada), the Discovery grants program of NSERC (Canada), CLS Graduate Student Travel Award (Canada) and to thank Drs. G. Belev & A. Webb of the CLS for their technical help and critical discussions.

References

Babin, P., Della Valle, G., Chiron, H., Cloetens, P., Hoszowska, J., Pernot, P., Reguerre, A.L., Salvo, L., Dendievel, R., 2008. In situ fast X-ray tomography study of the evolution of cellular structure in bread dough during proving and baking. In: Campbell, G.M., Scanlon, M.G., Pyle, L.D. (Eds.), Bubbles in Food 2: Novelty, Health and Luxury. Eagan Press, St. Paul, MN, USA, pp. 265–272.

Baker, J.C., Mize, M.D., 1941. The origin of the gas cell in bread dough. Cereal Chem. 18, 19–34.

Bellido, G.G., Scanlon, M.G., Page, J.H., Hallgrimsson, B., 2006. The bubble size distribution in wheat flour dough. Food Res. Int. 39, 1058–1066.

Campbell, G.M., Herrero-Sanchez, R., Payo-Rodriguez, R., Merchan, M.L., 2001. Measurement of dynamic dough density and effect of surfactants and flour type on aeration during mixing and gas retention during proofing. Cereal Chem. 78, 272–277.

Campbell, G.M., Rielly, C.D., Fryer, P.J., Sadd, P.A., 1998. Aeration of bread dough during mixing: effect of mixing dough at reduced pressure. Cereal Foods World 43, 163–167.

Campbell, G.M., Rielly, C.D., Fryer, P.J., Sadd, P.A., 1991. The measurement of bubble size distributions in an opaque food fluid. Trans. IChemE 69, 67–76.

Carlson, T., Bohlin, L., 1978. Free surface energy in the elasticity of wheat flour dough. Cereal Chem. 55, 539–544.

Carstensen, E.L., Foldy, L.L., 1947. Propagation of sound through a liquid containing bubbles. J. Acoust. Soc. Am. 19, 481–501.

Chichti, E., George, M., Delenne, J.-Y., Radjai, F., Lullien-Pellerin, V., 2013. Nano-mechanical properties of starch and gluten biopolymers from atomic force microscopy. Eur. Polym. J. 49, 3788–3795.

Commander, K.W., Prosperetti, A., 1989. Linear pressure waves in bubbly liquids: comparison between theory and experiments. J. Acoust. Soc. Am. 85, 732–746.

De Guio, F., Musse, M., Benoit-Cattin, H., Lucas, T., Davenel, A., 2009. Magnetic resonance imaging method based on magnetic susceptibility effects to estimate bubble size in alveolar products: application to bread dough during proving. Magn. Reson. Imaging 27, 577–585.

Elmehdi, H.M., Page, J.H., Scanlon, M.G., 2004. Ultrasonic investigation of the effect of mixing under reduced pressure on the mechanical properties of bread dough. Cereal Chem. 81, 504–510.

Fan, Y., 2007. Using Ultrasound to Investigate Relaxation and Resonance Phenomena in Wheat Flour Dough. University of Manitoba.

Fan, Y., Scanlon, M.G., Page, J.H., 2013. Influence of internal interfacial area on nanosecond relaxation of wheat gluten proteins as probed by broadband ultrasonic spectroscopy. Colloids Surface. B Biointerfaces 112, 466–473.

Koksel, F., Aritan, S., Strybulevych, A., Page, J.H., Scanlon, M.G., 2016a. The bubble size distribution and its evolution in non-yeasted wheat flour doughs investigated by synchrotron X-ray microtomography. Food Res. Int. 80, 12–18.

Koksel, F., Scanlon, M.G., 2012. Effects of composition on dough development and air entrainment in doughs made from gluten-starch blends. J. Cereal Sci. 56, 445–450.

Koksel, F., Scanlon, M.G., Page, J.H., 2016b. Ultrasound as a tool to study bubbles in dough and dough mechanical properties: a review. Food Res. Int. http://dx.doi.org/10.1016/j.foodres.2016.09.015.

Koksel, F., Strybulevych, A., Page, J.H., Scanlon, M.G., 2014. Ultrasonic characterization of unyeasted bread dough of different sodium chloride concentrations. Cereal Chem. 91, 327–332.

Leroy, V., Fan, Y., Strybulevych, A., Bellido, G.G., Page, J.H., Scanlon, M.G., 2008a. Investigating the bubble size distribution in dough using ultrasound. In: Campbell, G.M., Scanlon, M.G., Pyle, D.L. (Eds.), Bubbles in Food 2: Novelty, Health and Luxury. Eagan Press, St. Paul, MN, USA, pp. 51–60.

Leroy, V., Pitura, K.M., Scanlon, M.G., Page, J.H., 2010. The complex shear modulus of dough over a wide frequency range. J. Nonnewt. Fluid Mech. 165, 475–478.

Leroy, V., Strybulevych, A., Page, J.H., Scanlon, M.G., 2011. Influence of positional correlations on the propagation of waves in a complex medium with polydisperse resonant scatterers. Phys. Rev. E 83, 46605.

Leroy, V., Strybulevych, A., Page, J.H., Scanlon, M.G., 2008b. Sound velocity and attenuation in bubbly gels measured by transmission experiments. J. Acoust. Soc. Am. 123, 1931–1940.

Létang, C., Piau, M., Verdier, C., Lefebvre, L., 2001. Characterization of wheat-flour-water doughs: a new method using ultrasound. Ultrasonics 39, 133–141.

Mills, E.N.C., Wilde, P.J., Salt, L.J., Skeggs, P., 2003. Bubble formation and stabilization in bread dough. Trans. IChemE 81, 189–193.

Salerno, M., Zukowska, A., Thorat, S., Ruffilli, R., Stasiak, M., Molenda, M., 2014. High resolution imaging of native wheat and potato starch granules based on local mechanical contrast. J. Food Eng. 128, 96–102.

Shimiya, Y., Nakamura, K., 1997. Changes in size of gas cells in dough and bread during breadmaking and calculation of critical size of gas cells that expand. J. Texture Stud. 28, 273–288.

Strybulevych, A., Leroy, V., Scanlon, M.G., Page, J.H., 2007. Characterizing a model food gel containing bubbles and solid inclusions using ultrasound. Soft Matter 3, 1388–1394.

Strybulevych, A., Leroy, V., Shum, A.L., Koksel, H.F., Scanlon, M.G., Page, J.H., 2012. Use of an ultrasonic reflectance technique to examine bubble size changes in dough. IOP Conf. Ser. Mater. Sci. Eng. 42, 1–4.

Tanner, R., Dai, S., Qi, F., 2008. Bread dough rheology in biaxial and step-shear deformations. Rheol. Acta 47, 739–749.

Trinh, L., Lowe, T., Campbell, G.M., Withers, P.J., Martin, P.J., 2013. Bread dough aeration dynamics during pressure step-change mixing: studies by X-ray tomography, dough density and population balance modelling. Chem. Eng. Sci. 101, 470–477.

Upadhyay, R., Ghosal, D., Mehra, A., 2012. Characterization of bread dough: rheological properties and microstructure. J. Food Eng. 109, 104–113.

Wilson, P.S., 2005. Low-frequency dispersion in bubbly liquids. Acoust. Soc. Am. 6, 188–194.